Supplementary figures for ten Hacken et al. '*In vivo* modeling of CLL transformation to Richter's syndrome reveals convergent evolutionary paths and therapeutic vulnerabilities'

Supplementary figure S1

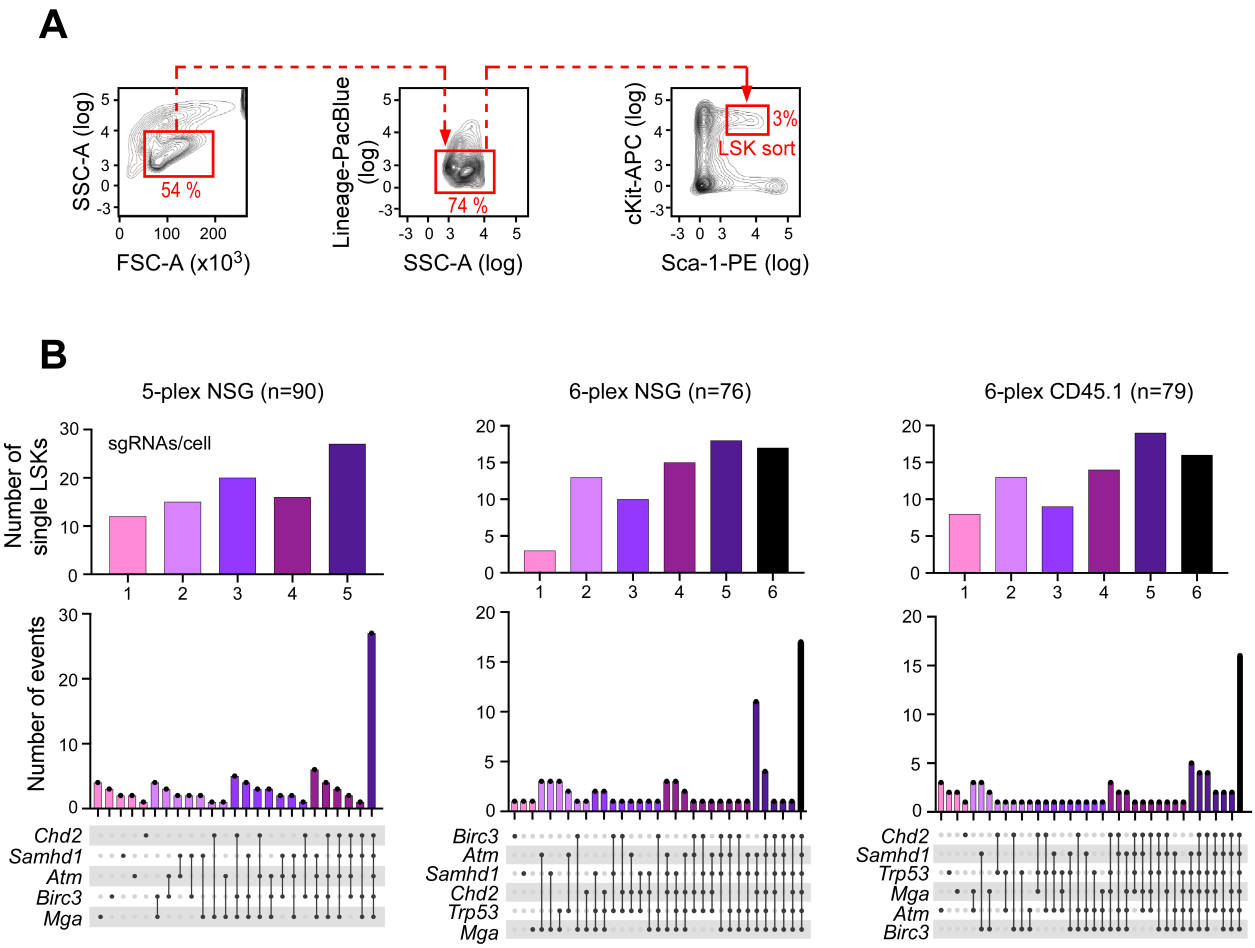

Supplementary figure S1. LSK sorting strategy and single-cell qPCR assessment of sgRNA abundance. A, LSK sorting strategy. **B**, Number of sgRNAs in individual LSKs from the targeting cohorts (upper panels), and related combinatorial sgRNAs assortments (lower panels), as identified by single cell qPCR analysis of individual LSKs from the 3 targeting cohorts. Total number of analyzed single LSKs is indicated in the figure.

Supplementary figure S2

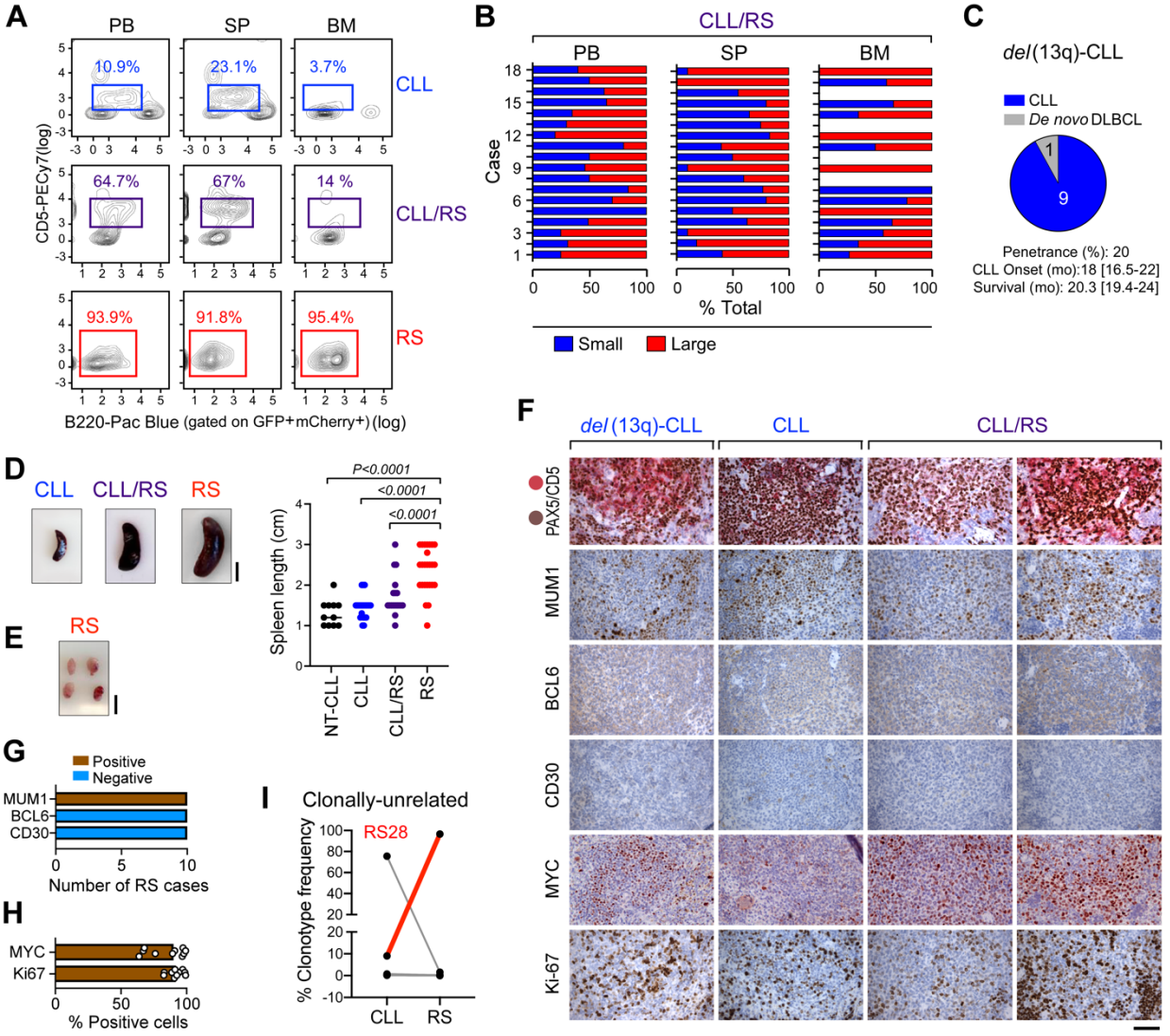

Supplementary figure S2. Pathologic features of the multiplexed mouse models. A, Representative flow cytometric plots highlighting presence of $B220^{+}CD5^{+}$ cells in one CLL, one CLL/RS and one RS case in the peripheral blood (PB), spleen (SP), and bone marrow (BM) at euthanasia. **B,** Small and large cell proportions (represented as % total lymphocytes) in the PB, SP, and BM of all 18 CLL/RS cases at euthanasia. **C,** Pie chart displaying number of total cases of *del*(13q)-CLL in a cohort of *del*(13q)-*Cd19*Cas9 transgenic animals. Overall penetrance, onset and survival (median and range) are indicated. **D,** Representative spleen from one CLL, one CLL/RS, and one RS case and spleen length (in cm) as analyzed at euthanasia in 11 NT-CLL, 21 CLL, 18 CLL/RS and 25 RS cases. Scale bar, 0.5 cm. *P* value, ANOVA with Tukey's correction for multiple comparisons. **E,** Image showing nodal enlargements in one representative RS case. Scale bar, 0.5 cm. **F,** Representative immunohistochemical staining from one *del*(13q)-CLL mouse, one case of multiplexed CLL, two cases of CLL/RS. Stains were performed for CD5/PAX5, MUM1, BCL6, CD30, MYC and Ki67. Images were taken at a 40x magnification, scale bar: 50µM. **G**, MUM1, BCL6 and CD30 IHC-based expression in 10 RS cases. **H,** MYC and

Ki67 quantification in 10 RS cases. **I**, Percent (%) clonotype frequency of shared BCR rearrangements as analyzed at time of CLL and upon RS transformation (euthanasia) in 1 RS case showing clonally-unrelated transformation. The dominant RS clonotype is shown in red.

Supplementary figure S3

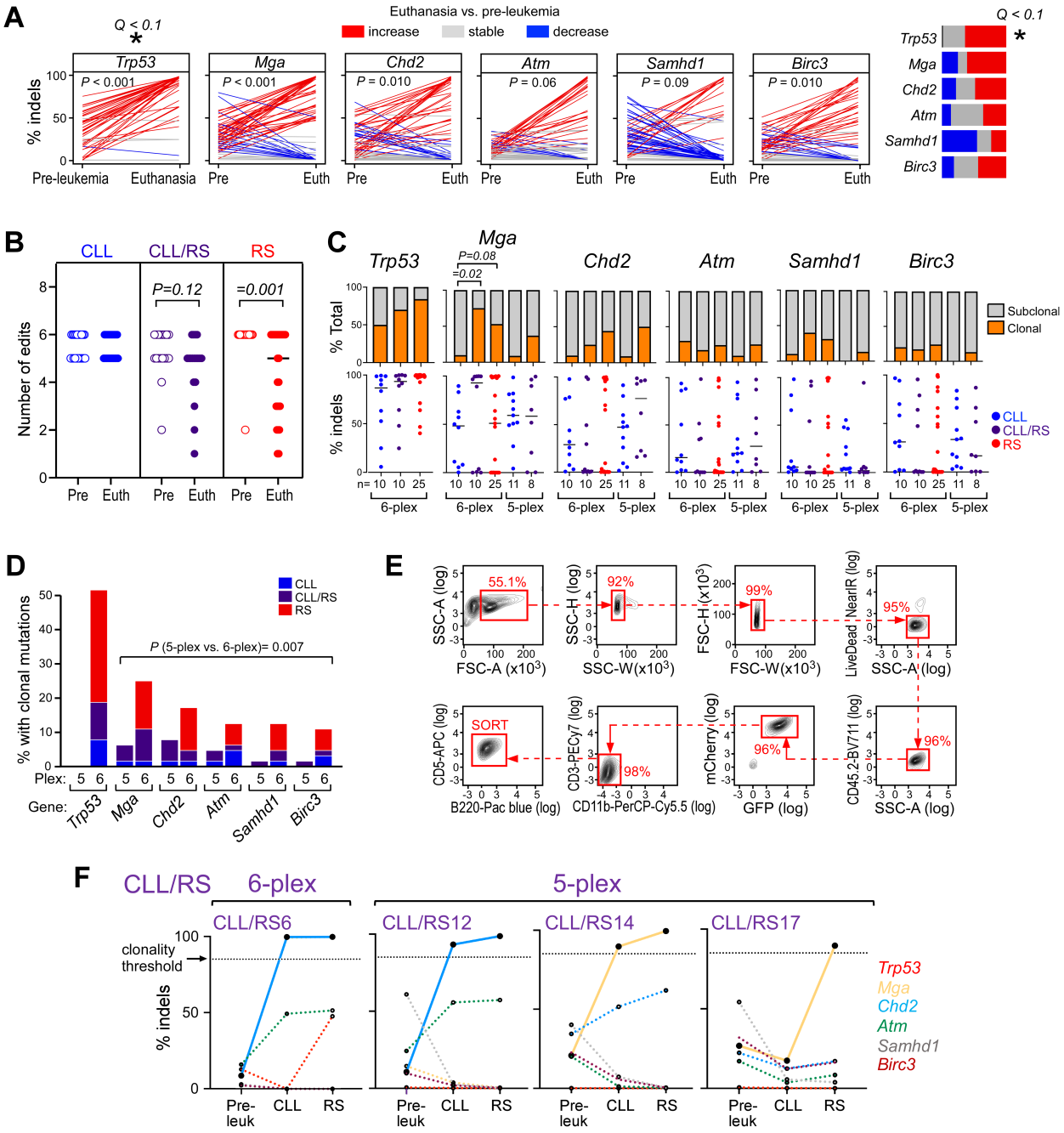

Supplementary figure S3. Clonal evolution analyses by combined CRISPR-seq and WGS. A, Comparison between % indels analyzed on pre-leukemic B cells and on tumor cells at euthanasia. Proportion of instances where the % indels increased (red), decreased (blue), or remained stable (grey) is shown (see **Methods** for statistical analysis). **B**, Number of gene edits in CLL, CLL/RS and RS cases at a pre-leukemic (4 months post-transplant) time point and at euthanasia. *P*, paired t test. **C,** The proportion in which a LOF driver is found as clonal or subclonal across the CLL (6-plex: 10 cases; 5-plex: 11), CLL/RS (6-plex: 10 cases; 5-plex:8), and 25 RS cases is provided (top), along with the individual % indels values (and group medians, horizontal lines) for each

sample across the 6 LOFs. *P* value, Fisher exact test comparing the proportions of clonal and subclonal events in CLL vs. CLL/RS or CLL vs. RS. **D,** Percent cases with clonal mutations in the 6 LOF lesions based on disease pattern (CLL, CLL/RS, RS) and transplant setting (6-plex, 5-plex) (*P* value, Fisher exact test comparing the cumulative number of clonal mutations in all genes except *Trp53* in the 6-plex vs. 5-plex cohorts). **E**, Example of flow sorting strategy of $GFP^{+}mCherry^{+}$ RS murine tumor samples. **F,** Longitudinal clonal trajectories of 4 CLL/RS cases as analyzed by CRISPR-seq. Clonality thresholds of 85% presence of indels are indicated by the horizontal dotted black line. *Mga* and *Chd2* trajectories are superimposed in sample CLL/RS6. Filled lines: clonal drivers; dotted lines: subclonal.

Supplementary figure S4

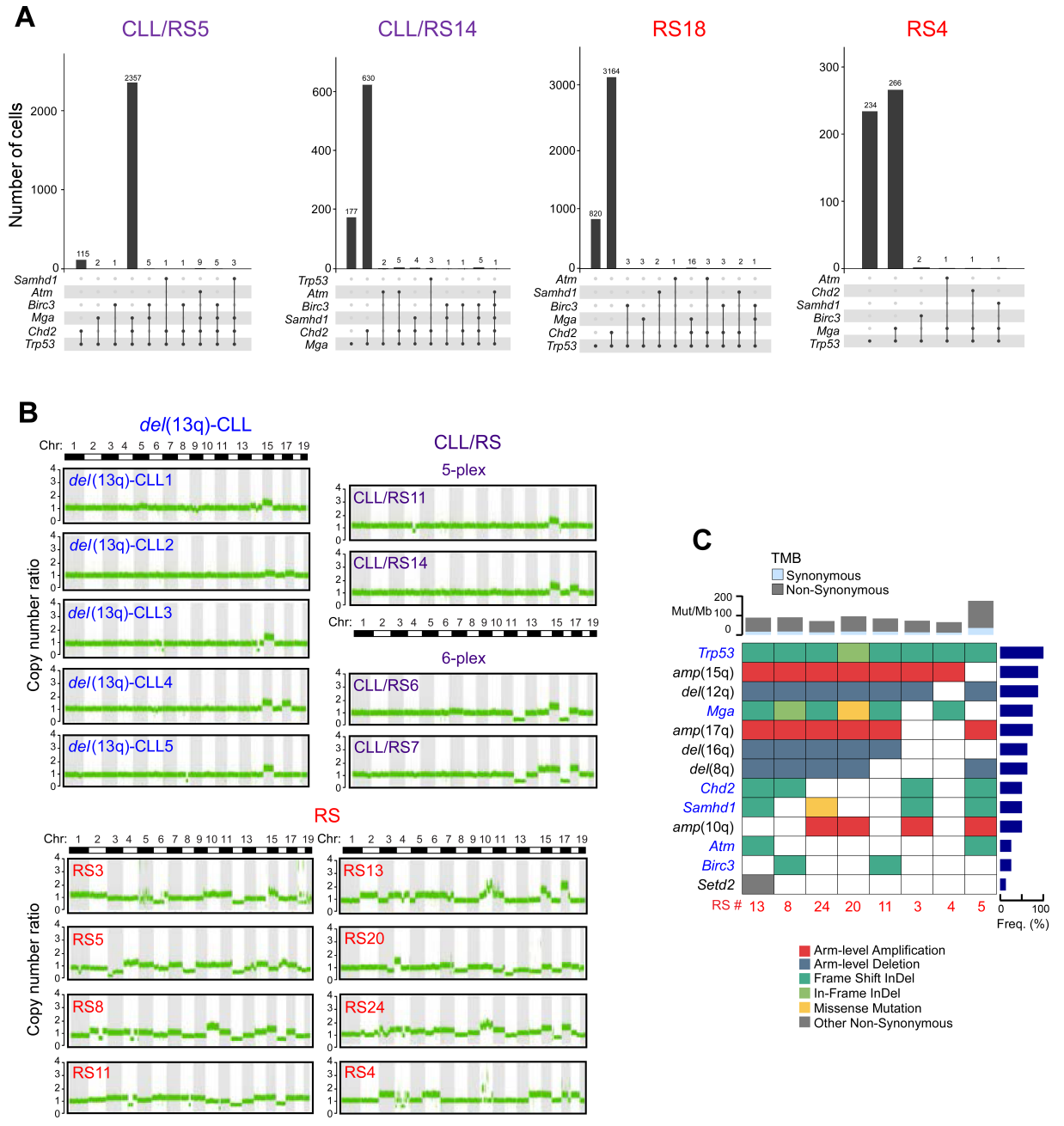

Supplementary figure S4. Single- cell DNA sequencing and whole genome sequencing analyses of murine tumors. A, Histogram showing the number of cells containing mutations for the indicated gene combinations, related to the single-cell DNA-seq analyses displayed in **Figure 3F**. **B,** Chromosomal copy-number variants in the 5 *del*(13q)-CLL, 2 CLL/RS 5-plex, 2 CLL/RS 6-plex and 8 RS samples assayed by WGS. The copy-number ratios to normal tissue are shown. **C,** Somatic mutations across 8 putative human driver genes along with recurrent copy number and single nucleotide variants are shown in the 8 RS cases that underwent WGS**.** Blue, CRISPR-edited genes; black, other alterations.

Supplementary figure S5

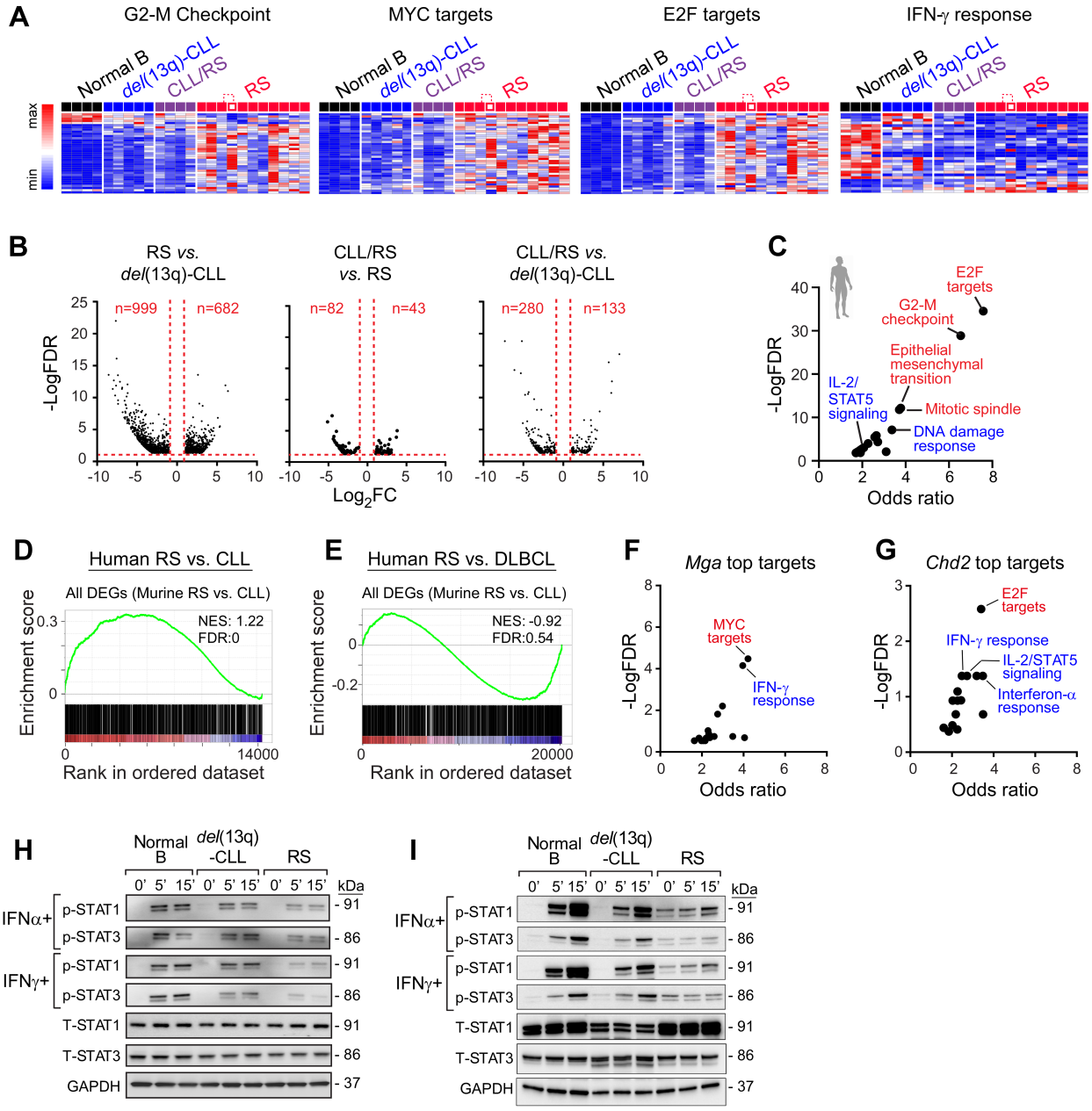

Supplementary figure S5. Transcriptome analyses of human and murine primary RS samples. A, Heatmaps of expression of genes involved in top differentially expressed functional categories across different murine samples. **B,** Volcano plots showing upregulated and downregulated groups across paired comparisons of *del*(13q)-CLL, CLL/RS and RS samples (FC>2, FDR<0.05). **C,** Pathways enriched for differentially expressed genes between human RS and CLL. Red, upregulated; blue, downregulated. **D,** Geneset enrichment plots showing correlation of murine RS vs. CLL in human RS vs. CLL data. DEGs: differentially expressed genes; NES, normalized enrichment score; FDR, false discovery rate. **E,** Geneset enrichment plots

showing correlation of murine RS vs. CLL in human RS vs. *de novo* DLBCL data. **F-G**, Pathways enriched for the top 500 targets of *Mga* or *Chd2*. Red, upregulated; blue, downregulated. **H-I,** Immunoblot analysis of phospho-STAT1 and STAT3 (and respective totals), after 5' and 15' stimulation with soluble IFNα and IFNγ. Two normal B cell, CLL and RS sample are shown. GAPDH was probed, as control.

Supplementary figure S6

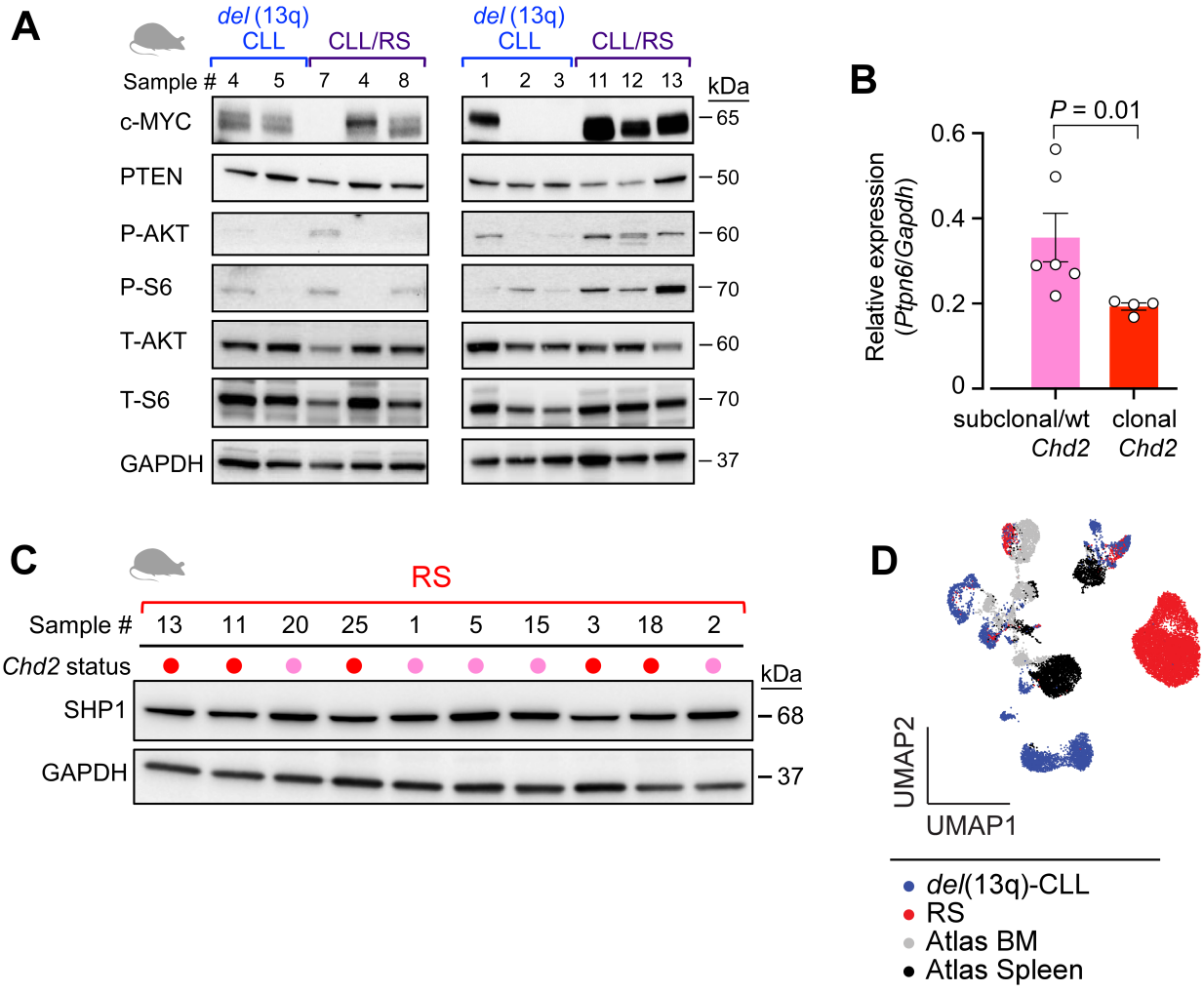

Supplementary figure S6. Transcriptomic, sc-ATAC-seq and immunoblot analyses on primary murine RS. A, Immunoblot analysis of 5 *del*(13q)-CLL and 6 CLL/RS murine tumors assessed for baseline expression of c-MYC, PTEN, and phosphorylation and total expression of AKT and S6 kinases. GAPDH is shown, as loading control. Separate gels, run concomitantly, were used for the analysis. **B**, Bar plot showing relative *Ptpn6*/*Gapdh* gene expression as analyzed by qPCR analysis. Mean with SEM is displayed. *P*, Mann Whitney. **C**, SHP1 protein expression analysis on 10 primary RS murine splenocytes carrying either wt/subclonal (pink) or clonal (red) *Chd2* mutations. Samples 15 and 3 are also displayed in **Figure 5E**. **D**, UMAP representation of 19,503 single cell chromatin accessibility profiles of circulating mononuclear cells from peripheral blood of *del*(13q)-CLL (blue) and RS (red), or from bone marrow (BM, grey) and spleen (black).

Supplementary figure S7

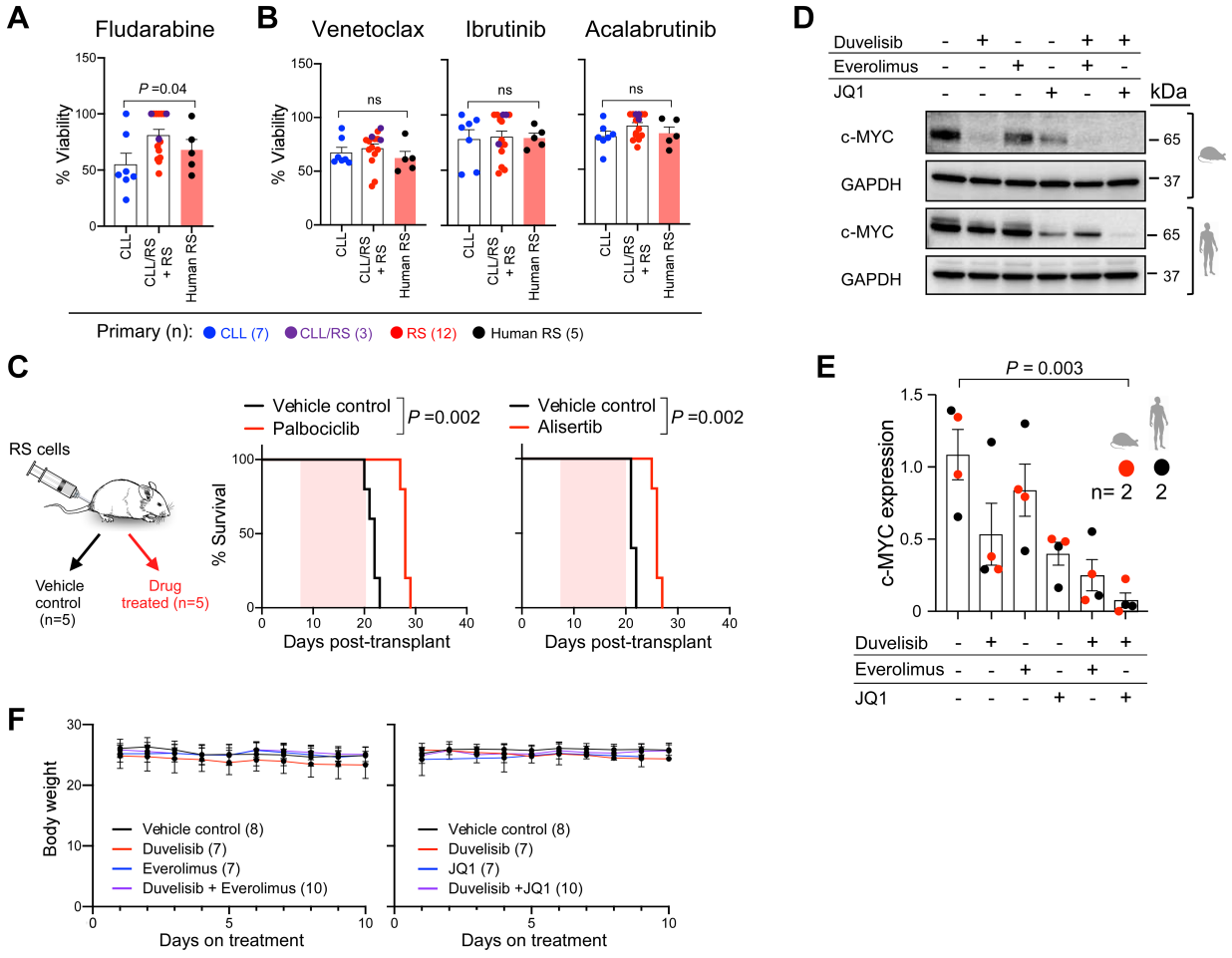

Supplementary figure S7. Drug treatment studies. A, Bar plots showing percent (%) viability after fludarabine treatment. Mean with SEM is displayed. *P* value, ANOVA. **B,** Dot plots showing percent (%) viability after venetoclax, ibrutinib, and acalabrutinib treatment. Mean with SEM is displayed. *P*, ANOVA. **C,** Transplant schema and survival curve of NSG mice transplanted with RS splenocytes and then treated with 50mg/kg palbociclib or 30mg/kg alisertib, for 2 weeks, followed by observation until survival endpoints. *P*, Log-rank test. The pink shaded area indicates the treatment period. **D**, Immunoblot assessment of c-MYC expression levels following a 12-hour treatment with single-agent duvelisib, everolimus, JQ1 or respective duvelisib-based combinations. One representative mouse and human samples are shown and GAPDH is used as loading control. **E**, Relative c-MYC/GAPDH expression as quantified by ImageJ on blots displayed in **Figure 6E** and **Figure S7D**. Mean with SEM is displayed. *P*, ANOVA. **F**, Daily body weight assessment of NSG mice throughout combinatorial treatment studies displayed in **Figure 6G**.